

Static and Dynamic Magnetic Properties of spin- $\frac{1}{2}$ Inequilateral Diamond-Chain Compounds $A_3\text{Cu}_3\text{AlO}_2(\text{SO}_4)_4$ ($A=\text{K}, \text{Rb}, \text{and Cs}$)

Katsuhiko Morita,^{1,*} Masayoshi Fujihala,² Hiroko Koorikawa,² Takanori Sugimoto,¹ Shigetoshi Sota,³ Setsuo Mitsuda,² and Takami Tohyama¹

¹*Department of Applied Physics, Tokyo University of Science, Tokyo 125-8585, Japan*

²*Department of Physics, Tokyo University of Science, Shinjuku, Tokyo 162-8601, Japan*

³*RIKEN Advanced Institute for Computational Science (AICS), Kobe, Hyogo 650-0047, Japan*

(Dated: October 6, 2018)

Spin- $\frac{1}{2}$ compounds $A_3\text{Cu}_3\text{AlO}_2(\text{SO}_4)_4$ ($A=\text{K}, \text{Rb}, \text{and Cs}$) have one-dimensional (1D) inequilateral diamond-chains. We analyze the temperature dependence of the magnetic susceptibility and determine the magnetic exchange interactions. In contrast to azurite, a dimer is formed on one of the sides of the diamond. From numerical analyses of the proposed model, we find that the dimer together with a nearly isolated 1D Heisenberg chain characterize magnetic properties including magnetization curve and magnetic excitations. This implies that a dimer-monomer composite chain without frustration is a good starting point for describing these compounds.

PACS numbers: 75.10.Jm, 75.10.Kt, 75.60.Ej

I. INTRODUCTION

Highly frustrated quantum magnets provide various exotic ground states such as gapless spin-liquid and gapped singlet dimer phases¹⁻³. In a magnetic field, the magnets exhibit magnetization plateaus because of the competition of frustration and quantum fluctuations. The typical constituent of frustrated magnets is a triangular unit of spin with antiferromagnetic (AFM) interaction for each bond. The spin- $\frac{1}{2}$ diamond-chain where the triangular unit is connected linearly thus is regarded as a typical highly frustrated system in one dimension⁴⁻⁶.

azurite $\text{Cu}_3(\text{CO}_3)_2(\text{OH})_2$ has originally been suggested to be a spin- $\frac{1}{2}$ distorted diamond-chain with AFM interactions for three bonds of a triangular unit⁷. A recent theoretical approach based on density functional theory together with numerical many-body calculations has proposed a microscopic model of azurite with less frustrated interactions⁸: Two of three Cu^{2+} spins are coupled strongly by AFM interaction J_2 [see Fig. 1(b)] to form a dimer singlet, whereas another spin consists of a monomer spin that is weakly connected to neighboring monomer spins by AFM interaction J_m , which has been indicated in the early stage of research in azurite⁷. This model, including the two energy scales of J_2 and J_m , has nicely reproduced the double-peak structures observed in the magnetic susceptibility (a peak at 5 K and a broad peak at 23 K)⁷ and the specific heat^{7,9}. In a magnetic field, the 1/3 magnetization plateau⁷ is interpreted as a result of almost fully polarized monomer spins and bounded dimer spins⁸. The model predicts a gapless low-energy spin excitation originating from a spin-liquid behavior due to an effective spin- $\frac{1}{2}$ Heisenberg chain¹⁰. However, three-dimensional magnetic interactions in azurite cause a magnetic order below 1.85 K.

Recently, a new highly one-dimensional (1D) diamond-chain compound $\text{K}_3\text{Cu}_3\text{AlO}_2(\text{SO}_4)_4$ has been reported¹¹. In this compound, the magnetic susceptibility exhibits a

double-peak structure similar to azurite, but the temperatures of the peaks (50 and 200 K) are one order of magnitude higher than those in azurite. Despite such high characteristic temperatures, there is no magnetic order down to 0.5 K, indicating a possible spin-liquid ground state¹¹. It is, thus, important to clarify common features characterizing the distorted diamond-chain compounds in both azurite and the new compound.

In this paper, we analyze the temperature dependence of the magnetic susceptibility in $\text{K}_3\text{Cu}_3\text{AlO}_2(\text{SO}_4)_4$ as well as newly synthesized compounds where Rb and Cs are substituted for K by using the finite-temperature Lanczos (FTL) method¹² and the exact diagonalization (ED) method. The estimated magnetic exchange interactions are found to form strong dimer bonds and monomer-monomer chains. This is similar to azurite, although the dimer-bond positions as well as their energy scales are different. The frustration is less effective in $\text{K}_3\text{Cu}_3\text{AlO}_2(\text{SO}_4)_4$ than in azurite, and the spin-liquid behavior at low temperatures is attributed to an effective spin- $\frac{1}{2}$ Heisenberg chain. Therefore, it is reasonable to conclude that diamond-chain compounds consisting of Cu^{2+} are less frustrated materials and thus a good starting point for the compounds is a dimer-monomer composite structure. Based on the estimated exchange interactions in $\text{K}_3\text{Cu}_3\text{AlO}_2(\text{SO}_4)_4$, we predict the magnetization curve with the 1/3 plateau and inelastic neutron-scattering spectrum by density matrix renormalization group (DMRG) calculations.

This paper is organized as follows. We describe the crystal structure of $A_3\text{Cu}_3\text{AlO}_2(\text{SO}_4)_4$ ($A = \text{K}, \text{Rb}, \text{and Cs}$) and discuss this effective model in Sec. II. In Sec. III, we analyze the temperature dependence of the magnetic susceptibility of $A_3\text{Cu}_3\text{AlO}_2(\text{SO}_4)_4$ and determine the magnetic exchange interactions. The magnetization curve and dynamical spin structure factor in $\text{K}_3\text{Cu}_3\text{AlO}_2(\text{SO}_4)_4$ are shown in Sec. IV. Finally, a summary is given in Sec. V.

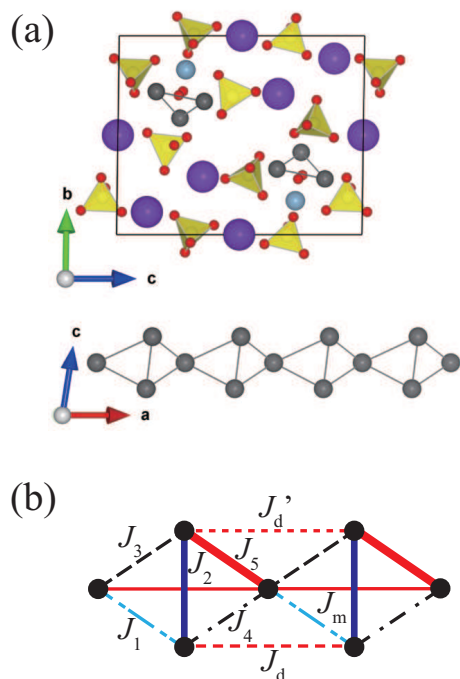


FIG. 1. (Color online) (a) Crystal structure of $A_3Cu_3AlO_2(SO_4)_4$ ($A = K, Rb, \text{ and } Cs$). The gray, purple, light blue, and red circles denote Cu, A, Al, and O atoms, respectively. The tetrahedrons with the red dots at the corners denote (SO_4) . The inequilateral diamond-chains run along the a axis. (b) Effective spin model of $A_3Cu_3AlO_2(SO_4)_4$. The circles represent Cu^{2+} ions with spin $1/2$. The blue broken, dark blue solid, black broken, black dashed-dotted, red thick solid, red thin solid, red dashed, and red dotted lines denote the exchange interactions J_1 , J_2 , J_3 , J_4 , J_5 , J_m , J_d , and J'_d , respectively.

II. CRYSTAL STRUCTURE AND MODEL

The crystal structure of $A_3Cu_3AlO_2(SO_4)_4$ is shown in Fig. 1(a). The diamond-chains composed of Cu^{2+} ions are formed along the a axis. Since the diamonds are inequilateral as discussed below, exchange interactions for the nearest-neighbor bonds [J_1 to J_5 as shown in Fig. 1(b)] are not necessarily the same. In addition, we consider exchange interactions connecting neighboring triangular units, denoted by J_m , J_d , and J'_d in Fig. 1(b). We note that only J_m is taken into account in azurite. In the present compounds there are possible paths for the J_d and J'_d bonds through SO_4 units. Since the surrounding components of the three J_m , J_d , and J'_d bonds are similar to each other, we assume that $J_m = J_d = J'_d$.

The effective spin Hamiltonian for $A_3Cu_3AlO_2(SO_4)_4$ under the external magnetic-field H is thus given by

$$\mathcal{H} = \sum_{\langle i,j \rangle} J_{ij} \mathbf{S}_i \cdot \mathbf{S}_j - g\mu_B H \sum_i S_i^z, \quad (1)$$

where \mathbf{S}_i is the spin- $\frac{1}{2}$ operator, J_{ij} is the exchange interaction corresponding to the bonds shown in Fig. 1(b), μ_B

is the Bohr magneton, and g is the gyromagnetic ratio.

Before fitting calculated magnetic susceptibilities to experimental ones, we need to roughly evaluate the value of exchange interactions. From the crystal structure analysis of $K_3Cu_3AlO_2(SO_4)_4$, the average Cu-O-Cu angle is estimated to be 104.7° , 95.2° , 102.5° , 105.8° , and 132.0° for the J_1 , J_2 , J_3 , J_4 , and J_5 bond, respectively¹³. Since the Cu-O-Cu angle significantly influences on the value of the exchange interactions¹⁴, the variation of the angles can give strong bond-dependent exchange interactions. According to the angle-dependent exchange interaction of cuprates¹⁴, J_5 with the largest angle is expected to be an AFM interaction with very roughly ~ 500 K, whereas J_2 with the smallest angle is to be ferromagnetic (FM) (~ -100 K). The values of the exchange interactions for other bonds are expected to be in between J_2 and J_5 . For simplicity, we take $J_1 = J_3 = J_4$ because of similar Cu-O-Cu angles. We emphasize that the side of the J_1 bond and the side of the J_5 bond, which are opposite sides of a diamond, are inequivalent. This means that the diamond is distorted making opposite sides inequivalent, i.e., an inequilateral diamond. We thus call $A_3Cu_3AlO_2(SO_4)_4$ the inequilateral diamond-chain compound.

III. MAGNETIC SUSCEPTIBILITIES

Taking into account this initial guess for the exchange interactions, we first investigate the temperature dependence of the spin susceptibility for $K_3Cu_3AlO_2(SO_4)_4$ by performing the FTL calculations for a 24-site diamond periodic chain [eight triangular units (the total number of site $N = 8 \times 3$)] together with the ED calculations for an 18-site diamond periodic chain. The calculated spin susceptibility χ is compared to the experimental data¹¹ obtained by subtracting the diamagnetic susceptibility χ_{dia} , the impurity-spin paramagnetic susceptibility χ_{imp} , and the Van Vleck paramagnetic susceptibility χ_{VV} ¹⁵ from the experimentally observed magnetic susceptibility. Figure 2(a) shows the experimental result (red solid line) and fitted results (black dashed line for $N = 24$ and brown dot-dashed line for $N = 18$) of χ for $K_3Cu_3AlO_2(SO_4)_4$. The parameter values are listed in Table I. With increasing system size from $N = 18$ to 24, the fitted results systematically approach the experimental one, indicating that the deviation from the experiment at $T < 70$ K is due to the finite size effect. We find that the double-peak structure is reproduced clearly: A broad peak at 200 K comes from large J_5 forming a dimer on the corresponding bond, whereas the low-temperature peak at 50 K is attributed to a 1D Heisenberg interaction with positive J_d being similar to the case of azurite. The other parameters only affect the heights of the two peaks. Since low-temperature χ for $N = 24$ below 30 K agrees with χ for an eight-site Heisenberg chain with the exchange interaction J_d , it is naturally expected that the low-temperature χ in experiment is reproduced by the exact χ for the 1D Heisenberg model. In fact, the Bethe-

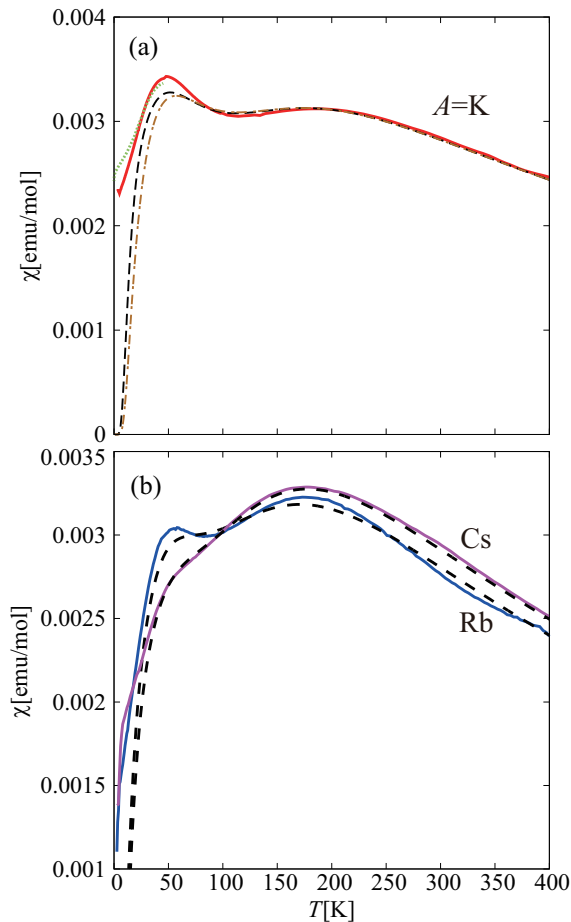


FIG. 2. (Color online) Temperature dependence of spin susceptibility in $A_3\text{Cu}_3\text{AlO}_2(\text{SO}_4)_4$ for (a) $A = \text{K}$ and (b) $A = \text{Rb}$ and Cs . The red solid lines show the experimental data. The black dashed lines represent the fitted data obtained by the FTL method for a 24-spin inequilateral diamond-chain. Note that the error of the FTL is within the width of the line. In (a), an ED result for an 18-spin chain is denoted by the brown dot-dashed line, and the Bethe-ansatz solution for the infinite Heisenberg chain is plotted by the green dotted line. The parameters are listed in Table I.

ansatz solution of the Heisenberg model¹⁷ shown as the dotted line in Fig. 2(a) well reproduces the experimental data, although some deviations probably due to the uncertainty of χ_{imp} remain.

The obtained value of J_5 is the largest and 15 times larger than the maximum interaction in azurite (~ 33 K). Similarly $J_d (= J'_d = J_m)$ in $A = \text{K}$ is 16 times larger than J_m in azurite (~ 4.62 K). Another important difference appears on the J_2 bond: J_2 is FM in $\text{K}_3\text{Cu}_3\text{AlO}_2(\text{SO}_4)_4$, whereas the dimer is located on the bond in azurite. It is also remarkable that there is only weak frustration in the diamond of $\text{K}_3\text{Cu}_3\text{AlO}_2(\text{SO}_4)_4$ since the magnitude of the FM J_4 interaction inducing frustration in a triangle is very small as compared with two other interactions J_2 and J_5 .

To confirm the magnetic interactions on A -site substi-

TABLE I. The exchange interactions and the gyromagnetic ratio obtained by fitting calculated χ to experimental ones.

A	$J_1 = J_3 = J_4$	J_2	J_5	$J_m = J_d = J'_d$	g
K	-30	-300	510	75	2.14
Rb	-17	-252	462	84	2.12
Cs	-19	-238	456	95	2.17

tuted compounds, we synthesized a single phase crystal with $A = \text{Rb}$ and Cs by a solid-state reaction in which high-purity A_2SO_4 , CuO , CuSO_4 and $\text{AlK}(\text{SO}_4)_2$ powder were mixed with a molar ratio of 1 : 2 : 1 : 1. The mixture was heated at 600°C for three days and then slowly cooled in air.

We fit calculated χ to the experimental ones for $A = \text{Rb}$ and Cs in Fig. 2(b). The two-peak structure is less pronounced but visible for $A = \text{Cs}$. From the estimated parameter values of the exchange interactions listed in Table I, we find that J_5 for $A = \text{Rb}$ and Cs is 10% smaller than that for $A = \text{K}$. Actually the broad peak position shifts to a lower temperature by nearly the same amount. In contrast, $J_d (= J'_d = J_m)$ increases from $A = \text{K}$ and Rb to Cs , inducing a slight shift of the low-temperature peak to a high-temperature peak. Other parameters with FM interactions reduce their magnitude from $A = \text{K}$ to Rb and Cs . These material-dependent changes in the interactions indicate a small change in Cu-O-Cu bond angles between K and Rb (Cs). A detailed crystal structure analysis will be necessary to confirm this and remains a future problem.

IV. MAGNETIZATION CURVE AND DYNAMICAL SPIN STRUCTURE FACTOR

To confirm the validity of the estimated exchange interactions, we calculate the magnetization curve for $\text{K}_3\text{Cu}_3\text{AlO}_2(\text{SO}_4)_4$ and compare it with available experimental data¹¹. The magnetization curve is calculated by DMRG for a $[N = 120 (= 40 \times 3)]$ -site periodic chain at zero temperature. The number of states kept in the DMRG calculation is $m = 300$, and the resulting truncation error is less than 2×10^{-6} . Figure 3 shows the calculated magnetization curve (red solid curve) as well as the experimental data (blue solid line) for a low magnetic field up to $H = 72$ T¹¹. The agreement with the experimental data is quite good. The magnetization near zero field is proportional to H , which is characteristic behavior in the 1D Heisenberg model and consistent with the fact that the low-energy scale is controlled by 1D interaction J_d as evidenced by good agreement with the exact magnetization curve (green dashed line) for the 1D Heisenberg model¹⁷. The calculated curve exhibits a magnetization plateau at the magnetization $M = 1/3$ as expected. The $1/3$ plateau starts from 108 T, which can be accessible by a pulse magnet experiment. Such an experiment is desired to confirm our proposed model. The

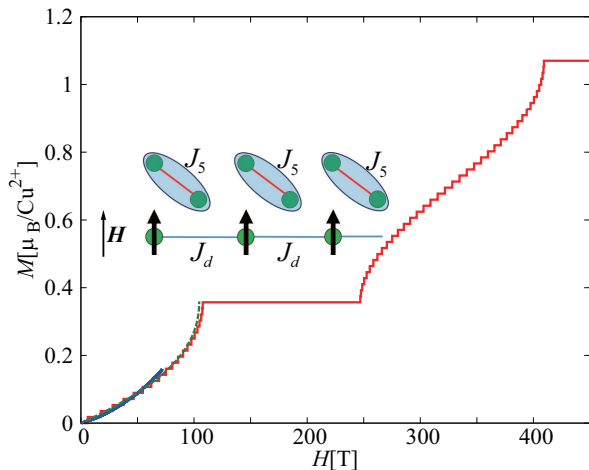


FIG. 3. (Color online) Magnetization curve for $\text{K}_3\text{Cu}_3\text{AlO}_2(\text{SO}_4)_4$. The red jagged solid line is a calculated curve by DMRG at zero temperature for a 120-site periodic chain with the exchange interactions estimated from χ . The blue solid line represents the experimental result under the magnetic field up to 72 T at 4.2 K¹¹. The green dashed line is the exact magnetization curve for the 1D Heisenberg model. The inset is a schematic of the spin configuration at the $1/3$ plateau with the dimers formed by J_5 and the 1D chain with J_d whose spins are ferromagnetically aligned with the direction of the applied magnetic field H .

calculated onset field of the $1/3$ magnetization plateau is 119 and 130 T for $A = \text{Rb}$ and Cs , respectively (not shown here). The slight increase in the onset field as compared with the $A = \text{K}$ case is attributed to the increase in J_d .

We also examine the dynamical spin structure factor for $\text{K}_3\text{Cu}_3\text{AlO}_2(\text{SO}_4)_4$, defined by

$$S(q, \omega) = -\frac{1}{\pi N} \text{Im} \langle 0 | S_{-q}^z \frac{1}{\omega - \mathcal{H} + E_0 + i\eta} S_q^z | 0 \rangle, \quad (2)$$

where q is the momentum for the triangular unit cell, $|0\rangle$ is the ground state with energy E_0 , η is a broadening factor, and $S_q^z = N^{-1/2} \sum_i e^{iqR_i} S_i^z$ with R_i being the position of spin i and S_i^z being the z component of \mathbf{S}_i . $S(q, \omega)$ is calculated by using the dynamical DMRG¹⁸ for a ($N=240$)-site periodic chain (80 triangular cells). The truncation number is $m = 400$, and the truncation error is less than 7×10^{-3} . The value of η is taken to be 0.65 meV.

Figure 4 shows the contour plot of $S(q, \omega)$. At the low-energy region below 10 meV, we find a clear dispersive behavior fitted quite well by $(\pi/2)J |\sin q|$ with $J = J_d$ (the red dashed line). This indicates that the lowest-energy branch comes from the 1D Heisenberg chain connected by the J_d bond. At the high-energy region around 40 meV, there is a dispersive structure having a minimum at $q = \pi$. This is nothing but the dispersion of a dimer predominantly formed on the J_5 bond. The dispersion relation is well reproduced by the second-order perturbation theory in terms of $J_m (= J'_d)$ giving a dispersion

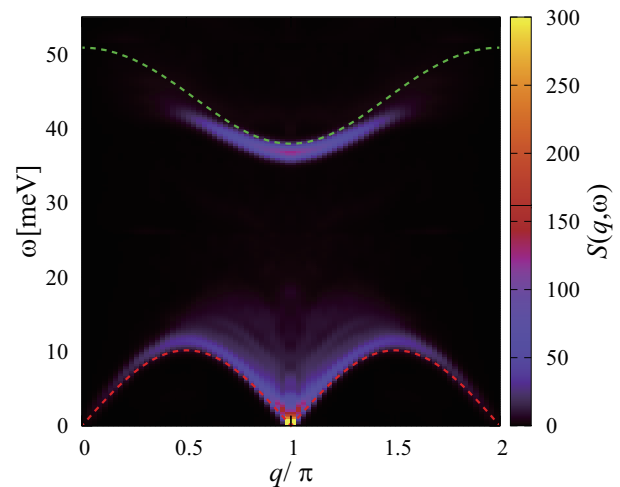


FIG. 4. (Color online) Dynamical spin structure factor $S(q, \omega)$ obtained by dynamical DMRG for a 240-site periodic chain with the exchange interactions for $\text{K}_3\text{Cu}_3\text{AlO}_2(\text{SO}_4)_4$. The red dashed line represents $(\pi/2)J |\sin q|$ with $J = J_d$, whereas the green dashed line represents $\omega_q = J_5 + J_m \cos q + \frac{1}{4} J_m^2 / J_5 (3 - \cos 2q)$.

of $\omega_q = J_5 + J_m \cos q + \frac{1}{4} J_m^2 / J_5 (3 - \cos 2q)$ (the green dashed line)^{19,20}, although there is a small deviation. Both the low-energy and high-energy structures should appear in inelastic neutron-scattering experiments. In fact, a preliminary experiment for the powder sample of $\text{K}_3\text{Cu}_3\text{AlO}_2(\text{SO}_4)_4$ has shown the corresponding structures¹³.

V. SUMMARY

We have examined the temperature dependence of the magnetic susceptibility for the inequilateral diamond-chain compound $A_3\text{Cu}_3\text{AlO}_2(\text{SO}_4)_4$ ($A = \text{K}, \text{Rb},$ and Cs) both experimentally and theoretically. The systematic analyses for $A = \text{K}, \text{Rb},$ and Cs clearly demonstrate that one of the bonds of the diamond has a strong AFM exchange interaction, producing a dimer. On the other hand, the bond shared by two triangles in the diamond is FM, in contrast to azurite where a dimer is formed on this bond. These behaviors are in accord with the angle dependence of the Cu-O-Cu bond. The dimer controls a high-temperature peak of the magnetic susceptibility as well as a high-energy dispersive structure in the dynamical spin structure factor. On the other hand, a low-energy peak in the magnetic susceptibility and low-energy excitations are controlled by monomers forming a 1D Heisenberg chain. Therefore, the dimer-monomer composite structure is a good starting point of diamond-type quantum spin compounds including azurites, in contrast to the original idea that the diamond-chain compounds are highly frustrated. Spin-liquid behaviors observed in the diamond-chain compounds thus are attributed to the presence of a 1D Heisenberg chain

formed by the monomers. In $A_3Cu_3AlO_2(SO_4)_4$, the magnetization curve with the 1/3 plateau and inelastic neutron-scattering spectra separated by the two energy scales are expected as theoretically demonstrated. Experiments to confirm these predictions are in progress.

ACKNOWLEDGMENTS

This work was supported, in part, by MEXT as a social and scientific priority issue (creation of new functional devices and high-performance materials to support next-generation industries (GCDMSI) to be tackled by using a post-K computer and by MEXT HPCI Strategic Programs for Innovative Research (SPIRE) (hp160222). The numerical calculation partly was carried out at the K Computer, Institute for Solid State Physics, The University of Tokyo and the Information Technology Center, The University of Tokyo. This work also was supported by Grants-in-Aid for Scientific Research (No. 26287079), Grants-in-Aids for Young Scientists (B) (No. 16K17753) from MEXT, Japan.

-
- * e-mail:katsuhiko.morita@rs.tus.ac.jp
- ¹ L. Balents, *Nature* **464**, 199 (2010).
 - ² *Introduction to Frustrated Magnetism*, edited by C. Lacroix, P. Mendels, and F. Mila, Springer Series in Solid-State Sciences (Springer, Berlin, 2011), Vol. 164.
 - ³ T. Imai and Y. S. Lee, *Phys. Today* **69**(8), 30 (2016).
 - ⁴ K. Takano, K. Kubo, and H. Sakamoto, *J. Phys.: Condens. Matter* **8**, 6405 (1996).
 - ⁵ K. Okamoto, T. Tonegawa, Y. Takahashi, and M. Kaburagi, *J. Phys.: Condens. Matter* **11**, 10485 (1999).
 - ⁶ K. Okamoto, T. Tonegawa, and M. Kaburagi, *J. Phys.: Condens. Matter* **15**, 5979 (2003).
 - ⁷ H. Kikuchi, Y. Fujii, M. Chiba, S. Mitsudo, T. Idehara, T. Tonegawa, K. Okamoto, T. Sakai, T. Kuwai, and H. Ohta, *Phys. Rev. Lett.* **94**, 227201 (2005).
 - ⁸ H. Jeschke, I. Opahle, H. Kandpal, R. Valentí, H. Das, T. Saha-Dasgupta, O. Janson, H. Rosner, A. Brühl, B. Wolf, M. Lang, J. Richter, S. Hu, X. Wang, R. Peters, T. Pruschke, and A. Honecker, *Phys. Rev. Lett.* **106**, 217201 (2011).
 - ⁹ K. C. Rule, A. U. B. Wolter, S. Süllow, D. A. Tennant, A. Brühl, S. Köhler, B. Wolf, M. Lang, and J. Schreuer, *Phys. Rev. Lett.* **100**, 117202 (2008).
 - ¹⁰ A. Honecker, S. Hu, R. Peters, and J. Richter, *J. Phys.: Condens. Matter* **23** 164211 (2011).
 - ¹¹ M. Fujihala, H. Koorikawa, S. Mitsuda, M. Hagihala, H. Morodomi, T. Kawae, A. Matsuo, and K. Kindo, *J. Phys. Soc. Jpn.* **84**, 073702 (2015).
 - ¹² J. Jaklič and P. Prelovšek, *Adv. Phys.* **49**, 1 (2000).
 - ¹³ M. Fujihala, H. Koorikawa, S. Mitsuda, K. Morita, T. Tohyama, K. Tomiyasu, A. Koda, H. Okabe, S. Itoh, T. Yokoo, S. Ibuka, M. Tadokoro, M. Itoh, H. Sagayama, R. Kumai, Y. Murakami, D. Nakamura, and S. Takeyama, arXiv:1705.01158.
 - ¹⁴ Y. Mizuno, T. Tohyama, S. Maekawa, T. Osafune, N. Motoyama, H. Eisaki, and S. Uchida, *Phys. Rev. B* **57**, 5326 (1998).
 - ¹⁵ χ_{dia} is estimated from¹⁶. χ_{imp} is assumed to be Curie-Weiss-type, i.e., $\chi_{\text{imp}} = n_{\text{imp}}C/(T)$, where C is the Curie constant for $S = 1/2$ and we set $n_{\text{imp}} = 0.017$. The Van Vleck paramagnetic susceptibility was estimated using $\chi_{\text{VV}} = (N\mu_B^2/\lambda)\Delta g = 9.42 \times 10^{-4} \Delta g$ emu/mol, where N is the number of Cu^{2+} ions, $\Delta g = g - g_e$ is the anisotropy of the gyromagnetic ratio, and $\lambda = 829 \text{ cm}^{-1}$ is the spin-orbit coupling coefficient of Cu^{2+} .
 - ¹⁶ G. A. Bain and J. F. Berry, *J. Chem. Educ.* **85**, 532 (2008).
 - ¹⁷ R.B. Griffiths, *Phys. Rev.* **133**, A768 (1964).
 - ¹⁸ S. Sota and T. Tohyama, *Phys. Rev. B* **82**, 195130 (2010).
 - ¹⁹ M. Reigrotzki, H. Tsunetsugu, and T. M. Rice, *J. Phys.: Condens. Matter* **6** 9235 (1994).
 - ²⁰ O. P. Sushkov and V. N. Kotov, *Phys. Rev. Lett.* **81**, 1941 (1998).